

1 **An integrated modelling approach for flood simulation in the**  
2 **urbanized Qinhuai River basin, China**

3

4 Runjie Li<sup>1,2</sup>, Jinkang Du<sup>1,2</sup>, Guodong Bian<sup>1,2</sup>, Yuefeng Wang<sup>3</sup>, Changchun Chen<sup>4</sup>,

5 Xueliang Zhang<sup>1,2</sup>, Maohua Li<sup>1,2</sup>, Shanshan Wang<sup>1,2</sup>, Senyao Wu<sup>1,2</sup>, Shunping Xie<sup>1,2</sup>,

6 Long Yang<sup>1\*</sup>, Chong-Yu Xu<sup>5</sup>

7

8 <sup>1</sup> School of Geography and Ocean Science, Nanjing University, Nanjing, Jiangsu Province

9 210023, China.

10 <sup>2</sup> Jiangsu Center for Collaborative Innovation in Geographical Information Resource

11 Development and Application, Nanjing, Jiangsu Province 210023, China.

12 <sup>3</sup> School of Geography and Tourism, Chongqing Normal University, Chongqing 401331,

13 China

14 <sup>4</sup> School of Geographical Sciences, Nanjing University of Information Science and

15 Technology, Nanjing, Jiangsu Province 210044, China

16 <sup>5</sup> Department of Geosciences, University of Oslo, PO Box 1047 Blindern, N-0316 Oslo,

17 Norway.

18 \* Corresponding author: E-mail address: [yanglong@nju.edu.cn](mailto:yanglong@nju.edu.cn) (L. Yang)

19 **Declarations**

20 **Funding**

21 This work was supported by the National Natural Science Foundation of China (No.

22 41771029 and No. 41371044), the Research Council of Norway (FRINATEK Project

23 274310) and the Strategic Priority Research Program of the Chinese Academy of  
24 Sciences (No. XDA23040202)

### 25 **Conflicts of interest**

26 The authors declare that they have no conflicts of interest.

### 27 **Availability of data and material**

28 The data that support the findings of this study are available from the corresponding  
29 author upon reasonable request.

### 30 **Code availability**

31 The code that supports the findings of this study is available from the corresponding  
32 author upon reasonable request.

### 33 **Authors' contributions**

34 All authors contributed to the study conception and design. Material preparation, data  
35 collection and analysis were performed by Runjie Li, Guodong Bian and Jinkang Du.

36 The first draft of the manuscript was written by Runjie Li, and all authors commented  
37 on previous versions of the manuscript. The modified manuscript was completed by  
38 Jinkang Du, Runjie Li and Long Yang. All authors read and approved the final  
39 manuscript.

### 40 **Acknowledgements**

41 This work was supported by the National Natural Science Foundation of China (No.  
42 41771029 and No. 41371044), the Research Council of Norway (FRINATEK Project  
43 274310), and the Strategic Priority Research Program of the Chinese Academy of  
44 Sciences (No. XDA23040202), whose support was greatly appreciated.

45 **Abstract**

46 The accurate simulation and prediction of flood response in urbanized basins remains  
47 a great challenge due to the spatial and temporal heterogeneities in land surface  
48 properties. We hereby propose an integrated modelling approach that consists of a semi-  
49 distributed conceptual hydrological model and a novel parameterization strategy. The  
50 modelling approach integrates the Xinanjiang (XAJ) model, Taihu Basin (TB) model,  
51 and Nash instantaneous unit hydrograph (IUH) into a framework. Model parameters  
52 are calibrated by optimizing their relationships with corresponding physical factors.  
53 The proposed modelling approach is applied in the Qinhuai River basin (QRB), China.  
54 The modelling approach shows satisfactory performance in flood simulation both for  
55 calibration and validation of flood events in the QRB. The approach has temporal and  
56 spatial prediction capability by using the established relationships between parameter  
57 values and physical factors. Robustness analysis reveals that the different sets of flood  
58 events used for parameter relationship calibration led to similar model performance.  
59 Numerical experiments show that impervious coverage poses strong influences on the  
60 model performance and needs to be considered in flood routing simulations for small-  
61 or medium-intensity flood events.

62 **Keywords**

63 Urbanization, Hydrological model, Model calibration, Flood response, Parameter  
64 estimation

## 65 **1. Introduction**

66 As one of the most extensive anthropogenic activities, urbanization has triggered a  
67 variety of environmental issues (Booth and Jackson 1997; Patra et al. 2018; Zhang et  
68 al. 2018), among which hydrological alterations have attracted increasing concern in  
69 the past several decades. Urban development increases impervious surface area and  
70 artificial drainage systems, which dramatically alter hydrological processes (Braud et  
71 al. 2013; Oudin et al. 2018; Schueler et al. 2009), such as an increase in surface runoff,  
72 a decrease in infiltration and changes in groundwater discharge (e.g., Burns et al. 2005;  
73 Salvadore et al. 2015). Previous studies have shown that disastrous flood events have  
74 become more frequent due to urbanization (Hu 2016; Hundedcha and Bardossy 2004).

75 Hydrological modelling is the most useful and effective tool to examine the  
76 impacts of urbanization on hydrological processes (Jacobson 2011; Trinh and Chui  
77 2013). Hydrological models can be typically divided into three categories: lumped,  
78 semi-distributed and distributed models (Arnold and Gibbons 1996; Bach et al. 2014;  
79 Salvadore et al. 2015). Of all three categories, semi-distributed models reasonably  
80 consider the spatial heterogeneity of subcatchments or hydrologic units compared with  
81 the lumped model. In addition, semi-distributed models are superior to distributed  
82 models in terms of reducing computational complexity and the number of parameters.  
83 Therefore, semi-distributed hydrological models are broadly employed in urban  
84 hydrological studies, e.g., the Storm Water Management Model (SWMM), Hydrologic  
85 Engineering Center-Hydrologic Modeling System (HEC-HMS), Soil and Water  
86 Assessment Tool (SWAT), and so on (e.g., Abbaspour et al. 2015; Arnold and Fohrer

87 2005; Lee and Heaney 2003; Lhomme et al. 2004; McColl and Aggett 2007; Valeo and  
88 Moin 2000; Zhao 1992).

89 In this study, we propose a semi-distributed conceptual modelling approach that  
90 combines the Xinanjiang (XAJ) model (Zhao 1992), Taihu Basin (TB) model (Cheng  
91 et al. 2006), and Nash instantaneous unit hydrograph (IUH) method (Nash 1960). The  
92 modelling approach uses spatially variable parameters and adopts conceptual methods  
93 to calculate runoff generation and routing. It has relatively feasible parameterization  
94 and high computational efficiency. Model calibration based on the observed  
95 hydrological data is necessary for obtaining better model performance. To reduce the  
96 number of calibrated parameters for semi-distributed models, parameters with low  
97 sensitivities or direct physical meanings can be assigned to their ‘typical’ value from  
98 current literature or field measurements. For example, hydraulic properties of soil can  
99 be obtained from the literature and from field measurements (Refsgaard 1997;  
100 Rodriguez et al. 2008). The ratio and connectivity of impervious surfaces can be  
101 obtained using remote sensing products (Lee and Heaney 2003). Parameters with high  
102 sensitivities are calibrated based on observed data. However, the observed data are  
103 usually scarce and unavailable for the calibration of parameters in each sub-basin. To  
104 determine the values of some highly sensitive parameters (especially for process-related  
105 parameters), one solution is to use regression equations to calculate those parameters  
106 based on physical data as independent variables (Xu 1999, 2003; Yang et al. 2018). For  
107 instance, Bedient and Huber (1992) presented regression equations for determining the  
108 time of concentration and the storage coefficient of the Clark unit hydrograph for each

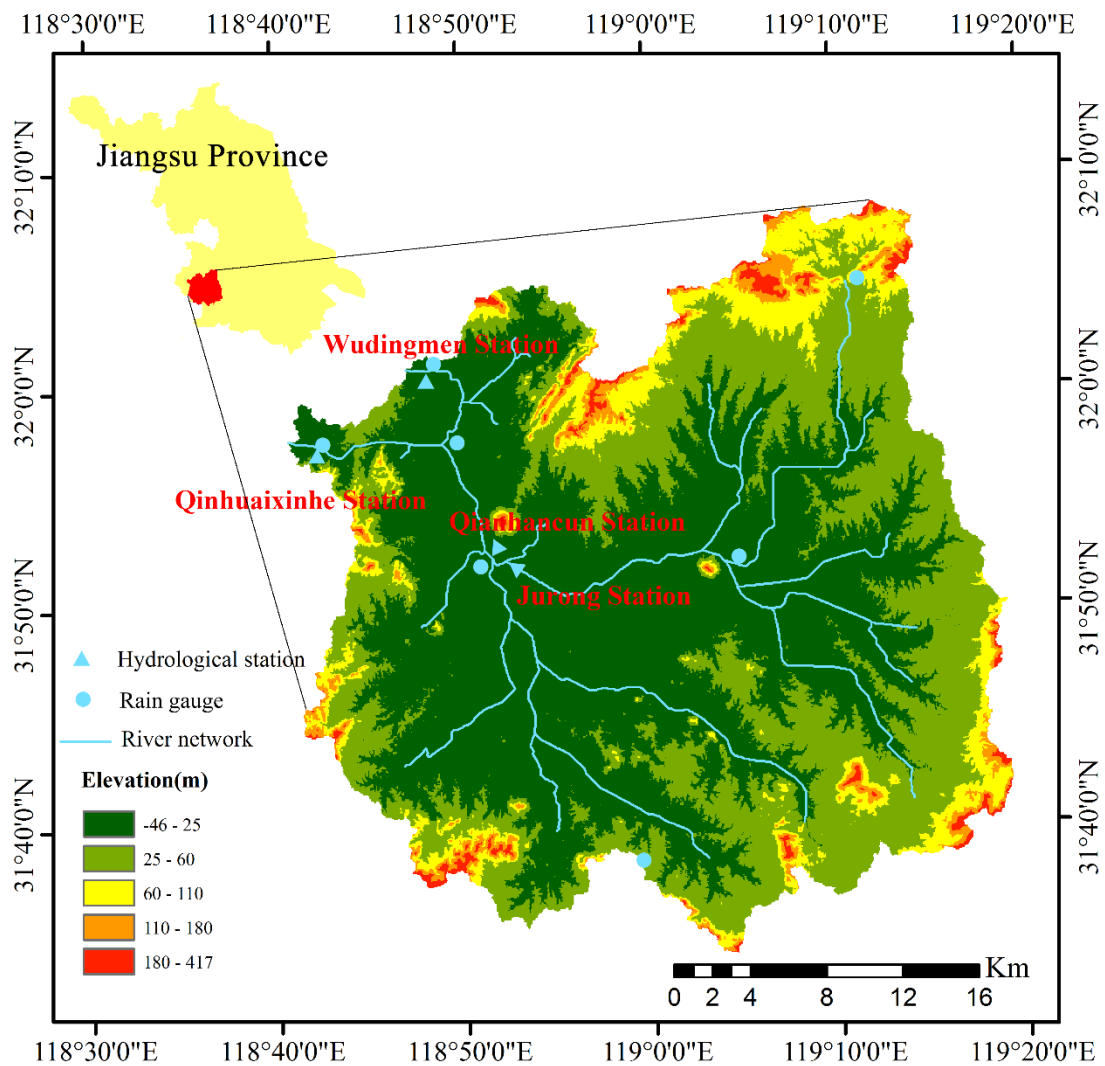
109 sub-basin. These equations represent relationships between parameters and other easily  
110 measurable physical factors, such as channel length, channel slope, and percentage of  
111 developed land. However, parameter estimations using these relationships are not  
112 always accurate because different basins or sub-basins may have different relationships;  
113 thus, the estimated values might be used only as initial values of the parameters for  
114 further calibration (USACE-HEC 2000). Ideally, these equations should be rebuilt or  
115 calibrated for each individual sub-basin. However, it is almost impossible to rebuild the  
116 equations due to the lack of observed data for each sub-basin. To address this problem,  
117 a parameterization scheme was proposed in this study by directly building unified  
118 equations to calculate parameters for each sub-basin, and the coefficients in the  
119 equations can be calibrated based only on the streamflow data at the basin outlet. In this  
120 way, the limitation of a lack of observation data for sub-basins can be solved, the  
121 number of calibrated model parameters can be reduced, and the calibration efficiency  
122 can be improved.

123 Therefore, the objectives of this study are to (1) propose a framework that uses a  
124 semi-distributed rainfall-runoff model for simulating flood processes in a mesoscale  
125 urbanized basin; (2) propose a parameterization scheme by establishing relationships  
126 between model parameters and potential driving factors; and (3) evaluate the simulation  
127 and prediction capacity of the integrated modelling approach.

## 128 **2. Study Area and Data**

129 The Qinhuai River basin (QRB) is located in Jiangsu Province, south-eastern China

130 (Fig. 1). The drainage area is 2,631 km<sup>2</sup>. The peak rainfall from June to August often  
 131 leads to severe flood hazards. Fast urbanization further increases the frequency of  
 132 floods in this region (Du et al. 2013). The main land-use types include water surface,  
 133 paddy land, urban land, dry land, and woodland. There are seven reservoirs, four  
 134 hydrological stations and seven rain gauges in the QRB. The Qinhuaixinhe and  
 135 Wudingmen hydrological stations are located at the outlet of the basin (see Fig. 1 for  
 136 locations).



137

138

**Fig. 1** Overview of the study area and location of hydrometeorological stations

139

Fourteen isolated flood events were selected from 1986 to 2015. The hourly

140 rainfall data for the seven rain gauges, the hourly discharge data from Qianhancun  
 141 Station and Jurong Station, and the instant peak flow and daily discharge data from  
 142 Wudingmen Station and Qinhuaijinhe Station for the flood events were collected from  
 143 the Nanjing Hydrological Bureau. The Thiessen polygon approach was used to  
 144 interpolate rainfall. The hourly outflows of Wudingmen Station and Qinhuaijinhe  
 145 Station were obtained by linear interpolation of the instant peak flow and the daily  
 146 discharge of the stations. The summary of rainfall at the basin scale and runoff observed  
 147 at Qianhancun station in the fourteen flood events is given in Table 1.

148 **Table 1** Summary of selected rainfall and runoff events

Storm no.	Storm date	Basin-scale rainfall			Streamflow at the Qianhancun Station	
		Depth (mm)	Duration (h)	Average intensity (mm/h)	Peak (m <sup>3</sup> /s)	Time to peak (h)
198707	July 2,1987	228.3	119	1.9	731	83
199106	June12,1991	333.9	115	2.9	964	81
199607	July 3, 1996	152.3	75	2.0	707	81
200607	July 19, 2006	171.4	91	1.9	513	79
200808	August 1,2008	115.3	32	3.6	654	37
200907	July 21, 2009	172.7	62	2.8	775	43
201007	July 12, 2010	153.2	32	4.8	491	34
201106	June 25, 2011	93.1	30	3.1	588	30
201107	July 18, 2011	95.6	56	1.7	517	30
201207	July 14,2012	62.8	17	3.7	380	20
201208	August 8,2012	78.3	37	2.1	667	47
201307	July 5,2013	125.9	62	2.0	497	37
201407	July 4, 2014	99.6	29	3.4	772	35
201506	June 16,2015	179.1	43	4.2	939	44

149 Fig. 2 shows changes in land use/land cover in the QRB during the period 1988-



150 2015. The land use/land cover was extracted from Landsat satellite images based on the  
151 rotation forest classifier method (Rodriguez et al. 2006; Bian et al. 2017). A noticeable  
152 change was found in the increase in impervious coverage from 3.92% to 19.76%, which  
153 was caused by the decrease in paddy field (from 50.09% to 29.94%) during the same  
154 period.

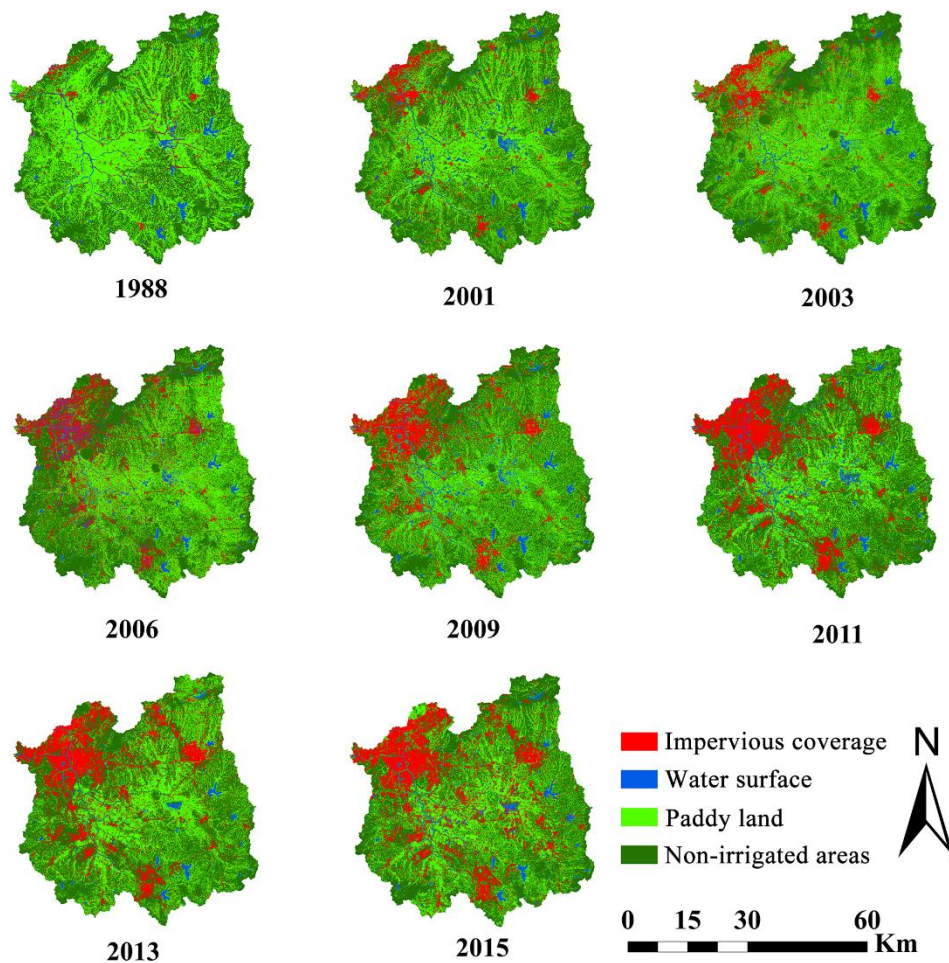


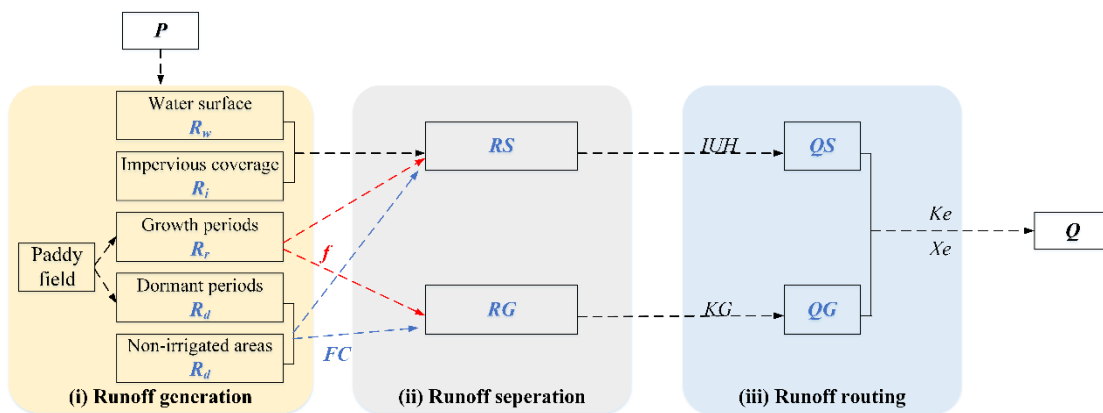
**Fig. 2** Land use classification results of the Qinhuai River basin

### 157 **3. Methodology**

#### 158 **3.1 Overview of the modelling framework**

159 The semi-distributed model has three individual modules: (i) runoff generation, (ii)

160 runoff separation, and (iii) runoff routing. The runoff generation module is derived from  
 161 the XAJ model and TB model; the runoff separation module is mainly adopted from the  
 162 XAJ model; and the runoff routing module is established based on the XAJ model using  
 163 the Nash IUH method (Nash 1957, 1960). The structure of the semi-distributed model  
 164 is given in Fig. 3. The key feature of the XAJ model is that runoff is generated and  
 165 calculated only when the soil moisture content reaches field capacity (Zhao et al. 1980).  
 166 The TB model is a hydrological modelling system that considers the heterogeneity in  
 167 runoff generation by categorizing land surfaces into four main categories, i.e., water  
 168 surface, urban, paddy field, and non-irrigated farmland (Cheng et al. 2006). The QRB  
 169 is divided into 18 sub-basins. The three modules were established for each of the sub-  
 170 basins.



171  
172 **Fig. 3** The structure of the semi-distributed hydrological model

### 173 3.1.1 Runoff generation

174 In the runoff generation module, four types of land uses are considered: water surface,  
 175 paddy field, impervious coverage, and non-irrigated areas.

176 The runoff generated from the water surface at each time interval is calculated as:

177 
$$R_w = P - \beta \times E_p \quad (1)$$

178 where  $R_w$  is the runoff generated from the water surface (mm),  $P$  denotes the  
 179 precipitation (mm),  $E_p$  denotes the potential evapotranspiration (mm), and  $\beta$  denotes the  
 180 adjustment factor of  $E_p$  (-).

181 Paddy fields can be divided into dormant periods and rice-growing periods. The  
 182 runoff generated from paddy fields is calculated in different rice-growing periods and  
 183 at each time interval, and it is described as:

184 
$$H_2 = P - \alpha \times E_p + H_1 - f \quad (2)$$

185 When  $H_2 > H_p$ ,

186 
$$R_r = H_2 - H_p, H_1 = H_p \quad (3)$$

187 When  $H_u < H_2 < H_p$ ,

188 
$$R_r = H_2 - H_u, H_1 = H_u \quad (4)$$

189 When  $H_d < H_2 < H_u$ ,

190 
$$R_r = 0, H_1 = H_2 \quad (5)$$

191 When  $H_2 < H_d$ ,

192 
$$R_r = H_2 - H_d, H_1 = H_d \quad (6)$$

193 where  $R_r$  is the runoff generated from the paddy field in the rice-growing period (mm)  
 194 at each time interval,  $\alpha$  represents the water requirement coefficient of the paddy field  
 195 (-),  $f$  is the infiltration in the paddy field (mm) at each time interval, and  $H_1$  and  $H_2$  are  
 196 the depths of water in the paddy field at the beginning and end of each time interval  
 197 (mm), respectively.  $H_p$  represents the depth of submergence tolerance (mm).  $H_u$  and  $H_d$   
 198 denote the suitable top and bottom depths of water needed at different growing periods

199 (mm), respectively.

200 The runoff generated from impervious coverage at each time interval is calculated  
201 as:

$$202 \quad R_i = \varphi \times P \quad (7)$$

203 where  $R_i$  is the runoff generated from impervious coverage (mm), and  $\varphi$  is the runoff  
204 coefficient (-).

205 The runoff generated from non-irrigated areas and dormant paddy fields at each  
206 time interval is estimated based on the XAJ model. In the saturated area where the soil  
207 moisture content reaches field capacity, the runoff is calculated using Eq. (8). Otherwise,  
208 the runoff calculation can be found by referring to Zhao (1992).

$$209 \quad R_d = P - (WM - W_o) - E \quad (8)$$

210 where  $R_d$  represents the runoff generation (mm) in the time interval,  $WM$  is the areal  
211 mean tension water capacity (mm),  $W_o$  is the initial soil water (mm), and  $E$  is the actual  
212 evapotranspiration (mm). Evapotranspiration is not considered in the runoff generation  
213 module due to its negligible contributions to flood simulation.

### 214 **3.1.2 Runoff separation**

215 Runoff separation aims to divide the generated runoff into two or more components  
216 according to land-use type. All the runoff generated from the water surface and  
217 impervious coverage would turn to surface runoff. The runoff from non-irrigated areas  
218 and dormant paddy fields is subdivided into surface runoff and groundwater runoff  
219 based on the free water capacity distribution curve (Li et al. 2018; Meng et al. 2016;

220 Zhao 1992), and the runoff in paddy fields calculated from Eqs. (2) to (6) turns to  
221 surface runoff; finally, infiltration at a steady rate contributes to groundwater runoff.  
222 For each sub-basin, the total surface runoff (groundwater runoff) is an area-weighted  
223 summation of runoff from the four land-use types (paddy land and non-irrigated areas).

### 224 **3.1.3 Runoff routing**

225 The surface runoff is routed directly to the outlet of each sub-basin by the Nash IUH  
226 method (Nash 1957, 1960), while the groundwater runoff is routed using the linear  
227 reservoirs method (Zhao et al. 1980; Zhao 1992). The discharge from the upper sub-  
228 basins is routed through the river network to the outlet of the sub-basin by the  
229 Muskingum successive-reaches model (Deng et al. 2009). The outflow at the outlet of  
230 each sub-basin is the summation of the surface runoff and groundwater discharge of the  
231 sub-basin and the river network routing discharge from the upper sub-basins.

### 232 **3.1.4 Reservoir operation**

233 Reservoirs can temporarily store flood water and release it later, which effectively  
234 lowers the magnitude and frequency of floods in downstream reaches. The changes in  
235 reservoir volume are simulated by the storage function approach as:

$$236 \quad \frac{dV}{dt} = INF - OF \quad (9)$$

237 where  $V$  is the reservoir storage ( $\text{m}^3$ ),  $t$  is the time (s),  $INF$  is the inflow ( $\text{m}^3/\text{s}$ ), and  $OF$   
238 is the release ( $\text{m}^3/\text{s}$ ). The details on reservoir operation can be found in Du et al. (2016).

### 239 **3.2 Model calibration strategy**

240 To reduce the number of calibrated parameters and improve the calculation efficiency  
241 of the model, the following parameterization strategy is proposed. (1) Parameters with  
242 low sensitivities or direct physical meanings are set to their ‘typical’ values based on a  
243 literature review and expert experience. (2) Parameters with high sensitivity are  
244 estimated based on the proposed parameterization scheme: calibrating relationships  
245 between parameters and influencing factors, such as urbanization index (impervious  
246 ratio) and basin characteristics (i.e., area, slope and length). (3) Other parameters are  
247 determined through calibration.

248 The parameters with high sensitivity and the typical values of most parameters in  
249 the proposed model can be found in the literature (e.g., Li et al. 2018; Lin et al. 2011;  
250 Meng et al. 2016; Zhao et al. 1980; Zhao 1992). For the parameters with high sensitivity  
251 for groundwater routing, the Muskingum successive-reaches method and the runoff  
252 coefficient of the impervious surface are manually optimized based on the trial-and-  
253 error method. The parameters of the Nash IUH method for surface runoff routing for  
254 each sub-basin are calibrated by using the proposed parameterization scheme. To reduce  
255 parameter dimensions, we assume that the Nash IUH parameters of all sub-basins have  
256 the same functional relationships with sub-basin characteristics (e.g., area, slope and  
257 length of the river network) and urbanization index (i.e., impervious rate), and the  
258 relationships between the Nash parameters, urbanization index and basin characteristics  
259 can be expressed as follows:

$$260 \quad n = f_1(A, SL, LE, IM, \dots) \quad (10)$$

261 
$$k = f_2(A, SL, LE, IM, \dots) \quad (11)$$

262 where  $f_1$  and  $f_2$  are functions;  $n$  and  $k$  are the number and storage coefficient of linear  
263 reservoirs of the Nash IUH, respectively; and  $A$ ,  $SL$ ,  $LE$ , and  $IM$  denote the  
264 characteristics of the area, slope, length, and impervious ratio of a sub-basin,  
265 respectively. The Nash IUH parameters of each sub-basin can be calculated based on  
266 the relationships. Parameter optimization thus turns into the optimization of functions  
267 (10) and (11). The best mathematical forms of relationships  $f_1$  and  $f_2$  could be obtained  
268 by maximizing the average NSE for all calibrated flood events. The enumeration  
269 optimal method or other optimal methods could be implemented to find the optimal  
270 parameters for each relationship by maximizing the average NSE. The proposed  
271 parameterization strategy can improve model calibration efficiency by reducing the  
272 number of calibrated parameters.

### 273 **3.3 Temporal and spatial prediction capabilities of the integrated modelling** 274 **approach**

275 To test the temporal prediction capability of the approach, six flood events from 1987  
276 to 2009 were used for the relationship calibration, while eight flood events from 2010  
277 to 2015 were used for model validation. Flood records from Qianhancun Station were  
278 used. The proxy-basin test was performed to verify the spatial prediction capability of  
279 the approach, i.e., calibrate flood events on one catchment and validate them on another  
280 catchment. The relationships of Nash IUH parameters were calibrated using the  
281 discharge data for fourteen flood events at Qianhancun Station. The calibrated

282 relationships were then used to predict flood events for the entire QRB.

### 283 3.4 Evaluation criteria

284 Four criteria were employed to evaluate the model performance (McCuen et al. 2006):  
285 the Nash-Sutcliffe efficiency (NSE), the coefficient of determination ( $R^2$ ), the relative  
286 error of peak discharge ( $D_p$ ) and the relative error of runoff volumes ( $D_v$ ), and they are  
287 calculated as follows:

$$288 \quad NSE = 1.0 - \frac{\sum_{i=1}^n [Q_c(i) - Q_o(i)]^2}{\sum_{i=1}^n [Q_o(i) - Q_o]^2} \quad (12)$$

$$289 \quad R^2 = \frac{\sum_{i=1}^n [Q_o(i) - Q_o] \times [Q_c(i) - Q_c]}{\sqrt{\sum_{i=1}^n [Q_o(i) - Q_o]^2} \times \sqrt{\sum_{i=1}^n [Q_c(i) - Q_c]^2}} \quad (13)$$

$$290 \quad D_p(\%) = \frac{Q_{p,c} - Q_{p,o}}{Q_{p,o}} \times 100\% \quad (14)$$

$$291 \quad D_v(\%) = \frac{\sum_{i=1}^n Q_c(i) - \sum_{i=1}^n Q_o(i)}{\sum_{i=1}^n Q_o(i)} \times 100\% \quad (15)$$

292 where  $Q_c(i)$  and  $Q_o(i)$  denote the estimated and observed discharges for time period  $i$   
293 ( $m^3/s$ ), respectively;  $Q_c$  and  $Q_o$  represent the estimated and observed mean values ( $m^3/s$ ),  
294 respectively;  $n$  is the total number of observed discharges; and  $Q_{p,c}$  and  $Q_{p,o}$  are the peak  
295 discharges of the estimated and observed hydrographs ( $m^3/s$ ), respectively.

## 296 4. Results and Discussion

### 297 4.1 Model calibration and validation



298 **4.1.1 Calibration of model parameters**

299 The runoff generation parameters over paddy land were set to suggested values and are  
 300 shown in Table 2 (Cheng et al. 2006). The parameters depend on different paddy  
 301 growing periods. The daily infiltration capacity was set to 1 mm due to the high  
 302 groundwater level and saturated soil during the growing season. The runoff coefficient  
 303 of impervious coverage was set to 0.65 (-). The parameters  $WM$  and  $W_0$  for non-irrigated  
 304 areas were set to 120 (mm) and 30 (mm), respectively. The daily recession coefficient  
 305 of groundwater in the linear reservoir method was set to 0.9, and the Muskingum time  
 306 constant and weighting factor were calibrated to be 2 (h) and 0.2, respectively. The best  
 307 relationships of the Nash IUH model parameters for all sub-basins were obtained by  
 308 maximizing the average NSE of calibrated flood events using the optimal enumeration  
 309 method:

310 
$$n = 0.6 \times A^{0.05} \times IM^{-0.01} \quad (16)$$

311 
$$k = 1.0 \times A^{0.27} \times IM^{-0.2} \quad (17)$$

312 where  $n$  and  $k$  are the number and storage coefficient of the Nash IUH of a selected sub-  
 313 basin,  $A$  is the area of the sub-basin, and  $IM$  is the impervious ratio of the sub-basin.

314 **Table 2** The runoff generation parameters of paddy land from Cheng et al. (2006)

Duration (day)	Depth of submergence tolerance (mm)	Top suitable water depth (mm)	Bottom suitable water depth (mm)	Coefficient of water requirement (-)	Daily infiltration capacity (mm)
5.16~5.25	20	10	5	1.00	1
5.26~6.23	30	20	10	1.00	1
6.24~6.30	50	30	20	1.35	1
7.1~8.4	50	30	20	1.30	1
8.5~9.3	50	40	30	1.65	1
9.4~9.16	50	30	20	1.76	1

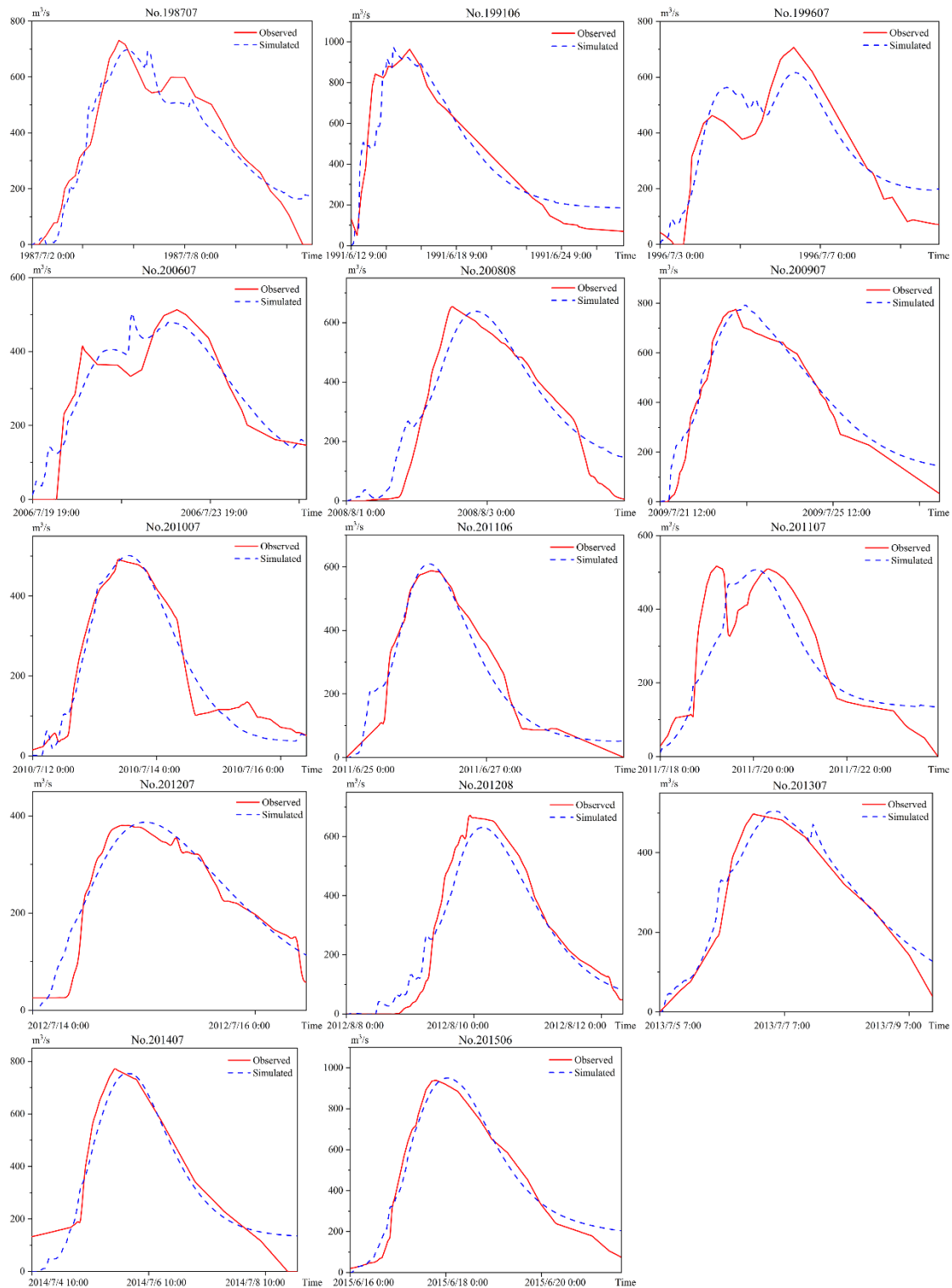
9.17~10.20	20	10	0	1.50	1
------------	----	----	---	------	---

### 315 4.1.2 Model performance

316 Table 3 indicates that the model achieves satisfactory performance during both  
317 calibration and validation periods, with the average values of  $R^2$  and NSE exceeding  
318 0.9 and the average values of  $D_p$  and  $D_v$  being lower than 5%. Fig. 4 demonstrates that  
319 the estimated results are well synchronized with the observed hydrographs in terms of  
320 both peak magnitudes and timing, indicating that the established model is applicable  
321 for flood simulation in the QRB. The parameterization strategy of calibrating  
322 relationships between model parameters and basin physical characteristics is also  
323 effective and suitable for the study basin.

324 **Table 3** The statistics of the model calibration and validation results at Qianhancun Station

Period	Flood code	Land-use pattern	Evaluation criteria			
			$R^2$	NSE	$D_p$ (%)	$D_v$ (%)
Calibration	198707	1988	0.91	0.91	4.65	1.24
	199607	2001	0.86	0.84	12.84	5.75
	200808	2009	0.92	0.90	2.44	7.84
	201106	2011	0.95	0.95	3.74	1.15
	201207	2013	0.93	0.92	1.84	4.42
	201407	2015	0.93	0.93	2.14	3.85
	Mean value			0.92	0.91	4.61
Validation	199106	1988	0.92	0.91	0.90	3.51
	200607	2006	0.88	0.87	1.96	4.00
	200907	2009	0.97	0.94	2.34	9.29
	201007	2011	0.96	0.95	2.05	4.39
	201107	2011	0.77	0.76	1.90	4.04
	201208	2013	0.97	0.96	5.43	3.84
	201307	2013	0.97	0.96	1.43	4.94
	201506	2015	0.97	0.97	1.17	3.42
Mean value			0.93	0.92	2.15	4.68



325

326

**Fig. 4** Observed and simulated hydrographs of 14 floods at Qianhancun Station

327

Table 4 shows the temporal prediction results at Qianhancun Station. The average

328

values of  $R^2$  and NSE of all predictive flood events exceeded 0.9, while the average

329

values of  $D_p$  and  $D_v$  were less than 5%, indicating that the proposed modelling approach

330 can achieve good temporal prediction capacity. It also demonstrates that the  
 331 relationships calibrated from the early period can be used for later or future flood event  
 332 prediction.

333 The statistics of the spatial prediction performance of the approach are shown in  
 334 Table 4. The results indicate satisfactory prediction results in terms of simulating flood  
 335 events in the whole QRB, with the average  $R^2$  and NSE exceeding 0.85 and the average  
 336 values of  $D_p$  and  $D_v$  being lower than 10%, which demonstrate that the calibrated  
 337 relationships over the upper and middle sub-basins can be transferred to the whole basin  
 338 for flood simulation.

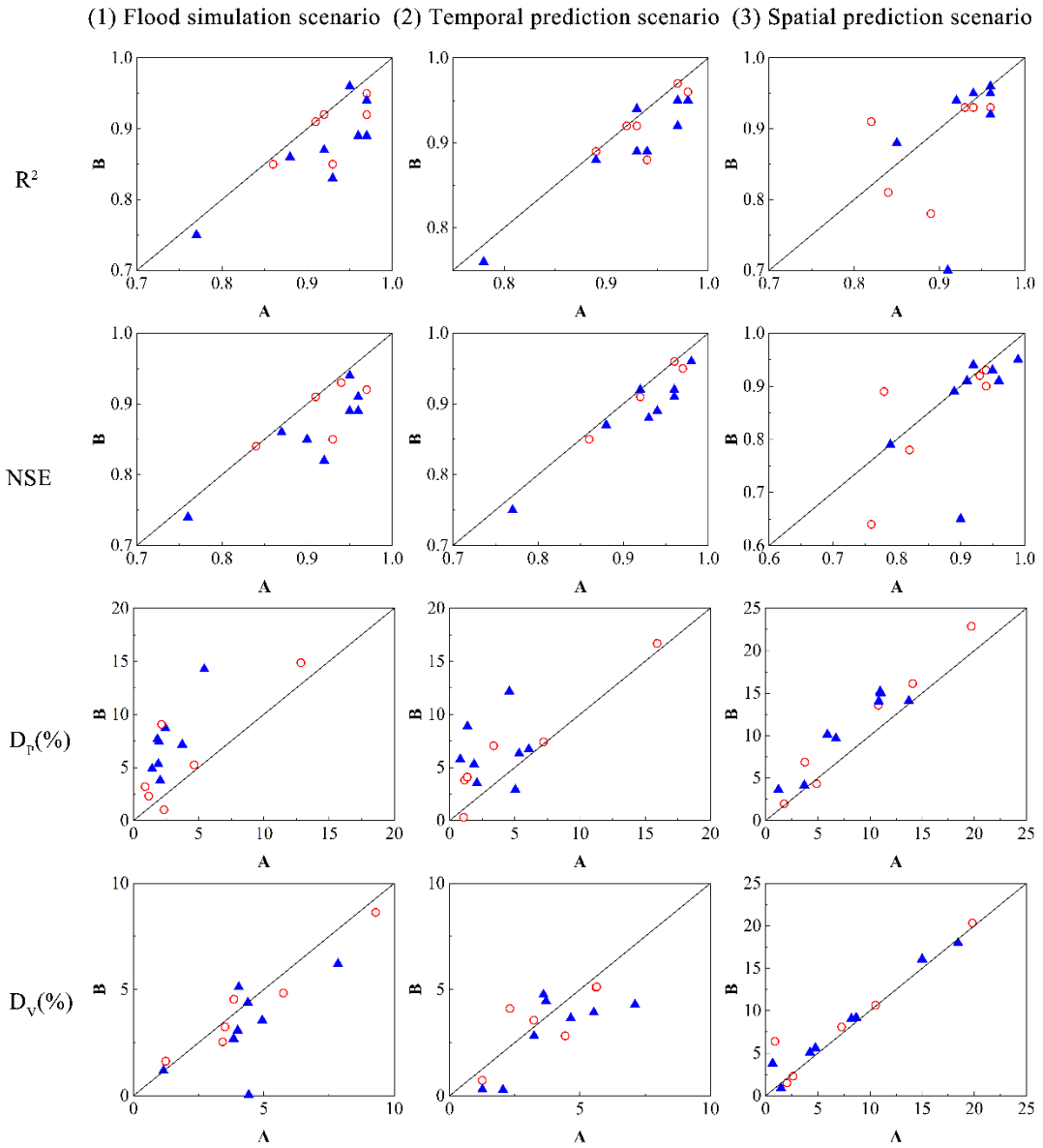
339 **Table 4** The statistics of model temporal prediction results at Qianhancun Station and spatial  
 340 prediction results in the whole QRB

Prediction capability	Flood code	Land-use pattern	Evaluation criteria			
			$R^2$	NSE	$D_p$ (%)	$D_v$ (%)
Temporal prediction results	201007	2011	0.94	0.94	0.82	1.26
	201106	2011	0.97	0.96	4.58	3.70
	201107	2011	0.78	0.77	2.10	3.60
	201207	2013	0.93	0.93	6.08	3.24
	201208	2013	0.98	0.98	1.37	2.05
	201307	2013	0.97	0.96	5.04	7.11
	201407	2015	0.94	0.93	3.38	2.31
	201506	2015	0.98	0.97	1.36	4.43
	Mean value		0.94	0.93	3.09	3.46
Spatial prediction results	198707	1988	0.94	0.94	3.76	2.03
	199106	1988	0.93	0.93	1.76	2.62
	199607	2001	0.84	0.82	4.88	7.27
	200607	2006	0.96	0.95	3.70	4.76
	200808	2009	0.92	0.92	6.73	4.24
	200907	2009	0.96	0.94	10.81	10.53
	201007	2011	0.96	0.96	13.72	1.47
	201106	2011	0.96	0.89	11.04	18.44
	201107	2011	0.85	0.79	10.85	15.00
	201207	2013	0.91	0.9	10.98	0.66
201208	2013	0.96	0.99	1.22	8.68	
201307	2013	0.94	0.91	5.92	8.22	
201407	2015	0.89	0.76	19.72	19.82	

201506	2015	0.82	0.78	14.09	0.88
Mean value		0.92	0.89	8.51	7.47

341 **4.2 Impacts of building relationships with or without the consideration of**  
342 **impervious areas on model performance**

343 The temporal and spatial variations of imperviousness should be considered in  
344 hydrological modelling for urbanized basins due to the role of impervious surface in  
345 influencing hydrological processes (Jacobson 2011; Praskievicz and Chang 2009).  
346 Previous studies have shown that an increase in impervious areas had large effects on  
347 the hydrological response for medium and small flood events but only small effects on  
348 extreme events (Braud et al. 2013; Kaspersen et al. 2015). To further examine the effects  
349 of impervious coverage on runoff generation and routing for flood events, the following  
350 test was conducted to determine the impacts of establishing the relationships of Nash  
351 IUH parameters with or without the consideration of imperviousness on model  
352 performances. Three scenarios were considered in the test: (1) flood simulation scenario;  
353 (2) temporal prediction scenario; and (3) spatial prediction scenario. The selected flood  
354 events for calibration and validation/prediction were the same as those described in  
355 Section 3.



356

357 **Fig. 5** Comparison of model simulation results, temporal prediction results and spatial prediction  
 358 results with (A) and without (B) the consideration of imperviousness. Blue triangles represent  
 359 small and medium floods (peak discharge lower than  $700 \text{ m}^3/\text{s}$ ), red circles represent large floods  
 360 (peak discharge higher than  $700 \text{ m}^3/\text{s}$ )

361 As seen from Fig. 5, almost all  $R^2$  and NSE values for floods without the  
 362 consideration of imperviousness in the surface runoff calculation are smaller than those  
 363 that consider imperviousness, while the values of  $D_p$  that consider imperviousness are  
 364 obviously smaller than those that do not consider imperviousness. For  $D_v$  values, all

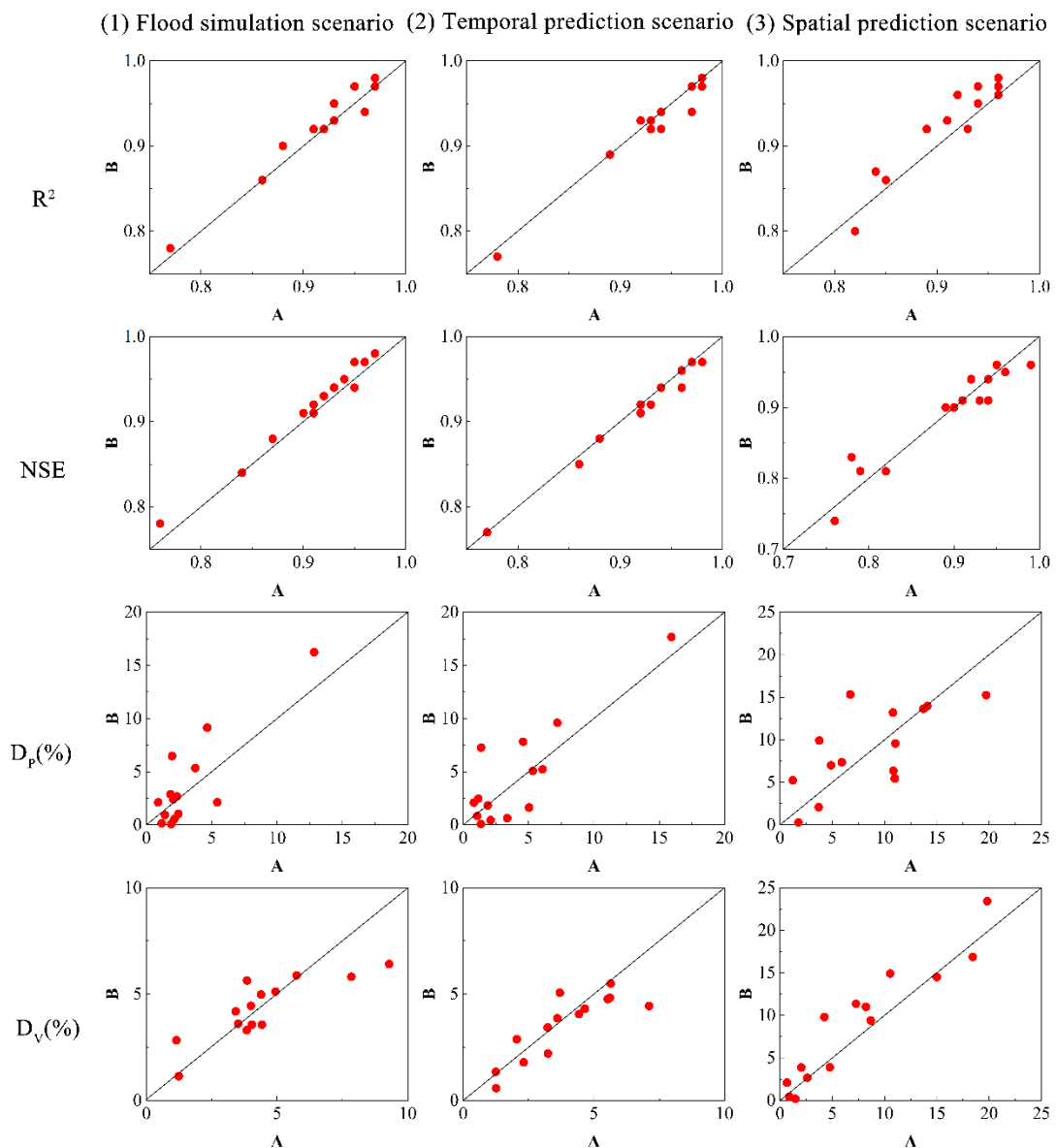
365 points are located near the 1:1 line, indicating that there is no distinct difference. This  
366 result is because impervious coverage only changes runoff-routing speed but not runoff  
367 volume. The volume of runoff generation remains the same for surface runoff routing  
368 regardless of whether imperviousness is considered.

369 For simulation and temporal prediction scenarios (Fig. 5), the values of  $R^2$ , NSE,  
370 and  $D_p$  for small and medium floods were considerably improved when imperviousness  
371 was considered compared to those that did not consider imperviousness, indicating that  
372 imperviousness has a pronounced impact on model simulation for small and medium  
373 flood events. For the spatial prediction scenario in the whole QRB (Fig. 5), the  
374 improvements in the  $R^2$ , NSE, and  $D_p$  values for most flood events were not as obvious  
375 as those in the first and second columns, which was likely because the impact of  
376 urbanization on the surface runoff process has been relatively weakened with the  
377 increase in basin size.

### 378 **4.3 Impacts of flood event selection for calibrating the relationships on model** 379 **performance**

380 The effects of using different flood events for calibrating relationships of Nash IUH  
381 parameters on model performance were also analysed. Three scenarios were built: (1)  
382 flood simulation scenario: six flood events different from the ones in Subsection 4.1  
383 were selected for relationship calibration, the others were used for validation, and the  
384 calibration and validation results were compared with those in Subsection 4.1; (2)  
385 temporal prediction scenario: three flood events from 1987 to 1996 were used for

386 calibration and the others were used for validation, the results were compared with  
 387 those calibrated by six flood events from 1987 to 2009 in Subsection 4.1; and (3) spatial  
 388 prediction scenario: the prediction results of the whole basin using relationships  
 389 calibrated by Qianhancun Station were compared with those calibrated by Jurong  
 390 Station.



391

392

**Fig. 6** Results of impacts of flood event selection for calibrating relationships on model

393

performance. (1) Flood simulation scenario: comparison of calibration and validation results by

394

selecting different flood events for calibration. *A* represents the previous flood simulations in



395 Subsection 4.1, and *B* represents flood simulations obtained by selecting the other six floods for  
396 relationship calibration; (2) Temporal prediction scenario: comparison of calibration and temporal  
397 prediction results obtained by selecting different flood events for calibration. *A* represents the  
398 previous calibration and temporal prediction results obtained by selecting the former six floods for  
399 relationship calibration in Subsection 4.1, and *B* represents those obtained by selecting the former  
400 three flood events for relationship calibration. (3) Spatial prediction scenario: comparison of  
401 spatial prediction results for the whole basin obtained by selecting different sub-basins for  
402 calibration. *A* represents the previous spatial prediction results with relationships calibrated by the  
403 discharge data of Qianhancun Station in Subsection 4.1, *B* represents the spatial prediction results  
404 with relationships calibrated by the discharge data of Jurong Station

405 As shown in Fig. 6, the  $R^2$ , NSE,  $D_p$ , and  $D_v$  values are located near the 1:1 line.  
406 The differences in the four criteria are statistically insignificant according to the *F*-test  
407 ( $\alpha=0.05$ , Jamshidian et al. 2007), indicating that the use of different flood events for  
408 parameter calibration yielded similar results for simulation and temporal prediction. In  
409 terms of spatial prediction, the relationships calibrated from different sub-basins could  
410 be transferred to the whole basin and generated similar spatial prediction results. These  
411 results demonstrate that the impact of flood event selection on model performance is  
412 insignificant, indicating that the proposed parameterization scheme of establishing  
413 unified relationships between model parameters and driving factors of sub-basins is  
414 robust for hydrological modelling in basins with urbanization. Thus, the relationships  
415 calibrated based on flood events with the corresponding land-use patterns can be  
416 effectively used for flood simulation and prediction under urbanization with certain  
417 reliability.

## 418 **5. Conclusions**

419 In this study, we proposed an integrated modelling approach to simulate flood events  
420 in the QRB, an urbanized basin of south-eastern China. The impacts of imperviousness  
421 on runoff generation and runoff routing were both taken into account. Considering the  
422 lack of observed data in sub-basins, unified relationships between Nash IUH model  
423 parameters and driving factors for all sub-basins were established and calibrated with  
424 observed data at the basin outlet. The following conclusions were obtained: (1) the  
425 proposed semi-distributed modelling approach can produce reasonable flood simulation  
426 results, especially when parameters of the Nash model for any sub-basin are calculated  
427 based on calibrated unified relationships between parameters and sub-basin physical  
428 characteristics; (2) imperviousness is an important factor that should be considered in  
429 flood routing calculations, especially for simulating small or medium floods; (3) the  
430 integrated modelling approach is effective, robust and efficient for flood simulation in  
431 mesoscale basins and has prediction capability over time and space for future land-use  
432 changes and adjacent basins. Future studies need to be carried out to extend the  
433 application of the proposed modelling approach to other urbanized basins.

## 434 **References**

- 435 Abbaspour KC, Rouholahnejad E, Vaghefi S, Srinivasan R, Yang H, Klove B (2015) A continental-scale  
436 hydrology and water quality model for Europe: Calibration and uncertainty of a high-resolution  
437 large-scale SWAT model. *Journal of Hydrology* 524:733-752.  
438 <https://doi:10.1016/j.jhydrol.2015.03.027>
- 439 Arnold CL, Gibbons CJ (1996) Impervious surface coverage - The emergence of a key environmental  
440 indicator. *Journal of the American Planning Association* 62:243-258.  
441 <https://doi:10.1080/01944369608975688>

442 Arnold JG, Fohrer N (2005) SWAT2000: current capabilities and research opportunities in applied  
443 watershed modelling. *Hydrological Processes* 19:563-572. <https://doi:10.1002/hyp.5611>

444 Bach PM, Rauch W, Mikkelsen PS, McCarthy DT, Deletic A (2014) A critical review of integrated urban  
445 water modelling-Urban drainage and beyond *Environmental. Modelling & Software* 54:88-107.  
446 <https://doi:10.1016/j.envsoft.2013.12.018>

447 Bedient PB, Huber WC (1992) *Hydrology and Floodplain Analysis*. Addison-Wesley, Massachusetts

448 Bian GD, Du JK, Song MM, Xu YP, Xie SP, Zheng WL, Xu CY (2017) A procedure for quantifying  
449 runoff response to spatial and temporal changes of impervious surface in Qinhuai River basin  
450 of southeastern China. *Catena* 157:268-278. <https://doi:10.1016/j.catena.2017.05.023>

451 Booth DB, Jackson CR (1997) Urbanization of aquatic systems: Degradation thresholds, stormwater  
452 detection, and the limits of mitigation. *Journal of the American Water Resources Association*  
453 33:1077-1090. <https://doi:10.1111/j.1752-1688.1997.tb04126.x>

454 Braud I et al. (2013) Evidence of the impact of urbanization on the hydrological regime of a medium-  
455 sized periurban catchment in France. *Journal of Hydrology* 485:5-23.  
456 <https://doi:10.1016/j.jhydrol.2012.04.049>

457 Burns D, Vitvar T, McDonnell J, Hassett J, Duncan J, Kendall C (2005) Effects of suburban development  
458 on runoff generation in the Croton River basin, New York, USA. *Journal of Hydrology* 311:266-  
459 281. <https://doi:10.1016/j.jhydrol.2005.01.022>

460 Cheng WH, Wang CH, Zhu Y (2006) *Taihu Basin Model*. Hohai University Press, Nanjing (in chinese)

461 Deng P, Li ZJ, Xie F (2009) Application of TOPMODEL in Buliu River catchment, Pearl River basin  
462 and comparison with Xin'anjiang model. *Journal of Lake Sciences* 21(3):441-444. (in chinese)

463 Du JK, Zheng DP, Xu YP, Hu SF, Xu CY (2016) Evaluating functions of reservoirs' storage capacities  
464 and locations on daily peak attenuation for Ganjiang River basin using Xinanjiang model.  
465 *Chinese Geographical Science* 26:789-802. <https://doi:10.1007/s11769-016-0838-6>

466 Du JK et al. (2013) Hydrological simulation by SWAT model with fixed and varied parameterization  
467 approaches under land use change. *Water Resources Management* 27:2823-2838.  
468 <https://doi:10.1007/s11269-013-0317-0>

469 Hu HB (2016) Rainstorm flash flood risk assessment using genetic programming: A case study of risk  
470 zoning in Beijing. *Natural Hazards* 83:485-500. <https://doi:10.1007/s11069-016-2325-x>

471 Hundecha Y, Bardossy A (2004) Modeling of the effect of land use changes on the runoff generation of

472 a river basin through parameter regionalization of a watershed model. *Journal of Hydrology*  
473 292:281-295. <https://doi:10.1016/j.jhydrol.2004.01.002>

474 Jacobson CR (2011) Identification and quantification of the hydrological impacts of imperviousness in  
475 urban catchments: A review. *Journal of Environmental Management* 92:1438-1448.  
476 <https://doi:10.1016/j.jenvman.2011.01.018>

477 Jamshidian M, Jennrich RI, Liu W (2007) A study of partial F tests for multiple linear regression models.  
478 *Computational Statistics & Data Analysis* 51:6269-6284.  
479 <https://doi:10.1016/j.csda.2007.01.015>

480 Kaspersen PS, Ravn NH, Arnbjerg-Nielsen K, Madsen H, Drews M (2015) Influence of urban land cover  
481 changes and climate change for the exposure of European cities to flooding during high-  
482 intensity precipitation. In: Rogger M et al. (eds) *Changes in Flood Risk and Perception in*  
483 *Catchments and Cities*, vol 370. *Proceedings of the International Association of Hydrological*  
484 *Sciences (IAHS)*. pp 21-27. <https://doi:10.5194/piahs-370-21-2015>

485 Lee JG, Heaney JP (2003) Estimation of urban imperviousness and its impacts on storm water systems.  
486 *Journal of Water Resources Planning and Management-Asce* 129:419-426.  
487 [https://doi:10.1061/\(asce\)0733-9496\(2003\)129:5\(419\)](https://doi:10.1061/(asce)0733-9496(2003)129:5(419))

488 Lhomme J, Bouvier C, Perrin JL (2004) Applying a GIS-based geomorphological routing model in urban  
489 catchments. *Journal of Hydrology* 299:203-216. <https://doi:10.1016/j.jhydrol.2004.08.006>

490 Li DC, Qu SM, Shi P, Chen XQ, Xue F, Gou JF, Zhang WH (2018) Development and integration of sub-  
491 daily flood modelling capability within the SWAT model and a comparison with XAJ model.  
492 *Water* 10. <https://doi:10.3390/w10091263>

493 Lin GY, Luo S, Shi YD, Gao Y (2011) Modification and verification of rice field runoff model under  
494 non-saturated soil condition. *Water Saving Irrigation* 10:33-36. (in chinese)

495 McColl C, Aggett G (2007) Land-use forecasting and hydrologic model integration for improved land-  
496 use decision support. *Journal of Environmental Management* 84:494-512.  
497 <https://doi:10.1016/j.jenvman.2006.06.023>

498 McCuen RH, Knight Z, Cutter AG (2006) Evaluation of the Nash-Sutcliffe efficiency index. *Journal of*  
499 *Hydrologic Engineering* 11:597-602. [https://doi:10.1061/\(asce\)1084-0699\(2006\)11:6\(597\)](https://doi:10.1061/(asce)1084-0699(2006)11:6(597))

500 Meng SS, Xie XH, Yu X (2016) Tracing temporal changes of model parameters in rainfall-runoff  
501 modeling via a real-time data assimilation. *Water* 8. <https://doi:10.3390/w8010019>

502 Nash JE (1957) The form of the instantaneous unit hydrograph. IASH Pub no. 45, 34:114-121

503 Nash JE (1960) A unit hydrograph study with particular reference to British catchments. Proc Inst Civ  
504 Eng, London 17:249-282

505 Oudin L, Salavati B, Furusho-Percot C, Ribstein P, Saadi M (2018) Hydrological impacts of urbanization  
506 at the catchment scale. Journal of Hydrology 559:774-786.  
507 [https://doi:10.1016/j.jhydrol.2018.02.064](https://doi.org/10.1016/j.jhydrol.2018.02.064)

508 Patra S, Sahoo S, Mishra P, Mahapatra SC (2018) Impacts of urbanization on land use/cover changes and  
509 its probable implications on local climate and groundwater level. Journal of Urban Management  
510 7:70-84. [https://doi:10.1016/j.jum.2018.04.006](https://doi.org/10.1016/j.jum.2018.04.006)

511 Praskievicz S, Chang H (2009) A review of hydrological modelling of basin-scale climate change and  
512 urban development impacts. Progress in Physical Geography 33:650-671.  
513 [https://doi:10.1177/0309133309348098](https://doi.org/10.1177/0309133309348098)

514 Refsgaard JC (1997) Parameterisation, calibration and validation of distributed hydrological models.  
515 Journal of Hydrology 198:69-97. [https://doi:10.1016/s0022-1694\(96\)03329-x](https://doi.org/10.1016/s0022-1694(96)03329-x)

516 Rodriguez F, Andrieu H, Morena F (2008) A distributed hydrological model for urbanized areas - Model  
517 development and application to case studies. Journal of Hydrology 351:268-287.  
518 [https://doi:10.1016/j.jhydrol.2007.12.007](https://doi.org/10.1016/j.jhydrol.2007.12.007)

519 Rodriguez JJ, Kuncheva LI, Alonso CJ (2006) Rotation Forest: A New Classifier Ensemble Method.  
520 IEEE Transactions on Pattern Analysis and Machine Intelligence 28(10):1619-30.  
521 [https://doi.org/ 10.1109/TPAMI.2006.211](https://doi.org/10.1109/TPAMI.2006.211)

522 Salvadore E, Bronders J, Batelaan O (2015) Hydrological modelling of urbanized catchments: A review  
523 and future directions. Journal of Hydrology 529:62-81.  
524 [https://doi:10.1016/j.jhydrol.2015.06.028](https://doi.org/10.1016/j.jhydrol.2015.06.028)

525 Schueler TR, Fraley-McNeal L, Cappiella K (2009) Is impervious cover still important? Review of recent  
526 research. Journal of Hydrologic Engineering 14:309-315. [https://doi:10.1061/\(asce\)1084-  
527 0699\(2009\)14:4\(309\)](https://doi.org/10.1061/(asce)1084-0699(2009)14:4(309))

528 Trinh DH, Chui TFM (2013) Assessing the hydrologic restoration of an urbanized area via an integrated  
529 distributed hydrological model. Hydrology and Earth System Sciences 17:4789-4801.  
530 [https://doi:10.5194/hess-17-4789-2013](https://doi.org/10.5194/hess-17-4789-2013)

531 USACE-HEC (2000) Hydrologic modeling system HEC-HMS, Technical Reference Manual. US Army

532 Corps of Engineers, Hydrologic Engineering Center, Davis, California

533 Valeo C, Moin SMA (2000) Grid-resolution effects on a model for integrating urban and rural areas.

534 Hydrological Processes 14:2505-2525. [https://doi.org/10.1002/1099-](https://doi.org/10.1002/1099-1085(20001015)14:14<2505::AID-HYP111>3.0.CO;2-3)

535 [1085\(20001015\)14:14<2505::AID-HYP111>3.0.CO;2-3](https://doi.org/10.1002/1099-1085(20001015)14:14<2505::AID-HYP111>3.0.CO;2-3)

536 Xu C-Y (1999) Estimation of parameters of a conceptual water balance model for ungauged catchments.

537 Water Resources Management 13:353-368. <https://doi.org/10.1023/a:1008191517801>

538 Xu C-Y (2003) Testing the transferability of regression equations derived from small subcatchments to

539 a large area in central Sweden. Hydrology and Earth System Sciences 7:317-324.

540 <https://doi.org/10.5194/hess-7-317-2003>

541 Yang X, Magnusson J, Rizzi J, Xu C-Y (2018) Runoff prediction in ungauged catchments in Norway:

542 comparison of regionalization approaches. Hydrology Research 49:487-505.

543 <https://doi.org/10.2166/nh.2017.071>

544 Zhang Y et al. (2018) Simulation and assessment of urbanization impacts on runoff metrics: Insights

545 from landuse changes. Journal of Hydrology 560:247-258.

546 <https://doi.org/10.1016/j.jhydrol.2018.03.031>

547 Zhao RJ (1992) The Xinanjiang model applied in China. Journal of Hydrology 135(1):371-

548 381.[https://doi.org/10.1016/0022-1694\(92\)90096-E](https://doi.org/10.1016/0022-1694(92)90096-E)

549 Zhao RJ, Zhang YL, Fang LR, Liu XR, Zhang QS (1980) The Xinanjiang model. Hydrological

550 Forecasting Proceedings Oxford Symposium, IASH 129, pp 351-356